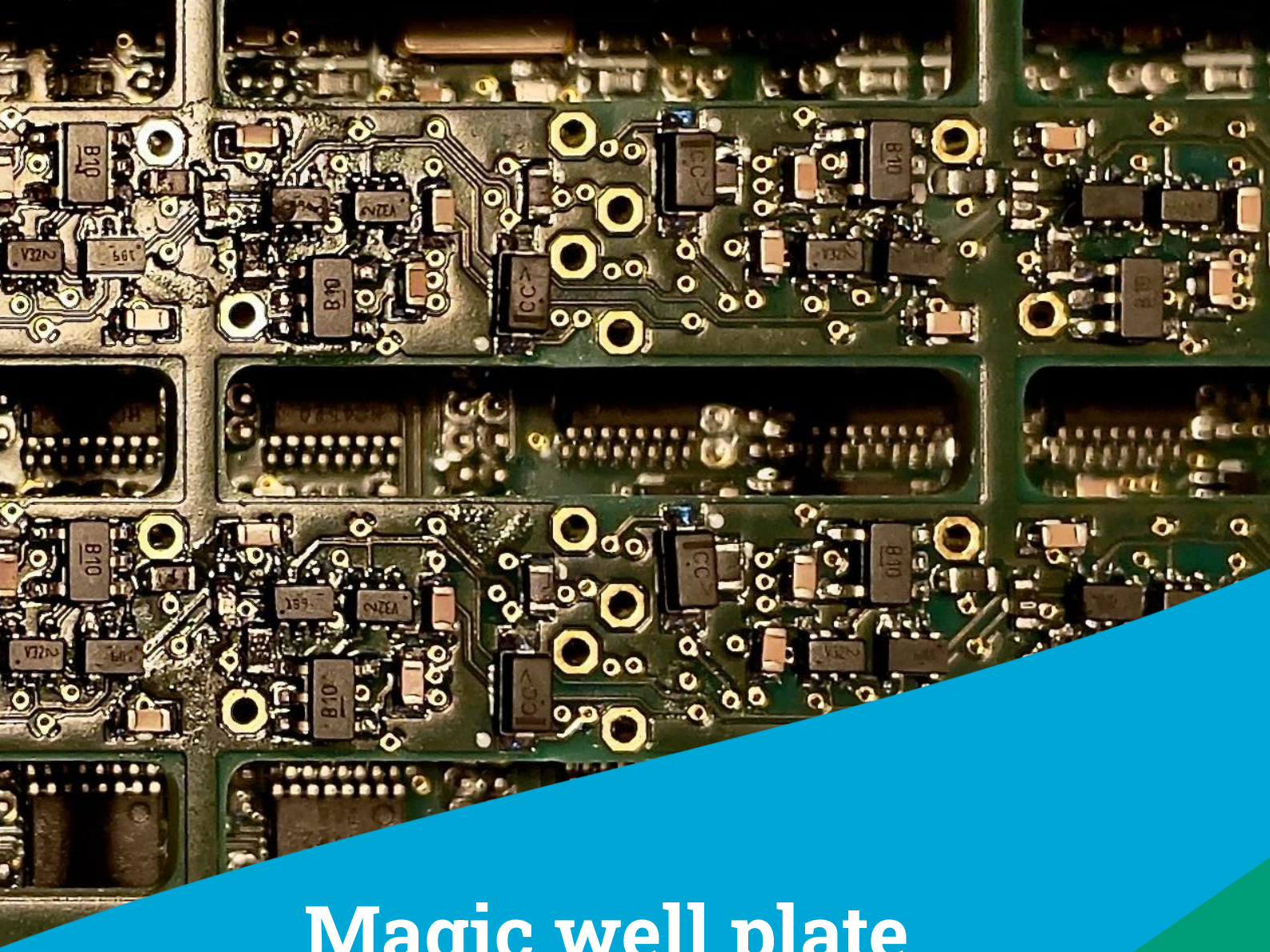

Magic well plate

For electric stimulation of cells

Author: Ryan Houtman
Date: 21/8/2025

TU Delft

High throughput electric stimulation circuitry for cellular biology

By

Ryan Houtman

In partial fulfilment of the requirements for the degree of:

Master of Science
in Electrical Engineering

at the Delft University of Technology,
to be defended publicly on Wednesday 27th of August.

Supervisors:	Dr. A. Savva,	
	Prof. dr. ir. W. A. Serdijn	
Thesis committee:	Dr. A. Savva,	TU Delft
	Prof. dr. ir. W. A. Serdijn,	TU Delft
	Dr. ir. M.A.P. Pertijs	TU Delft

TU Delft

Contents

Abstract

Electric stimulation can be used to get cells to behave in all kinds of ways. Examples include getting them to move, proliferate, excrete chemicals, or stop doing any of these things. However, finding the optimal stimulation parameters is a tedious process of trial and error which is made difficult by the equipment that is currently in use. It is often bulky, expensive and only allows for a limited number of experiments to be done simultaneously. To combat this issue, this work aims to create a circuit that allows the simultaneous stimulation of as many different channels of cells as possible without causing accidental damage to the cells through harmful electrochemical reactions. To this end, a printed circuit board is designed to fit underneath a 48-well plate. It can set the waveform timing to be a square wave with variable frequency, duty cycle and amplitude with different settings for the positive and negative part of stimulation. To create this device, research is done to the state of art of the current devices used to stimulate cells. As well as the viability of stainless-steel as a cheaper alternative reference electrode material with respect to platinum and Ag/AgCl electrodes. While the stimulation part of the design works, the charge balancing circuit does not and requires more work.

1 Introduction

The body and by extension cells in the body are electrically active. Not only the neurons and their action potentials but also the cell membrane voltage and voltage gradients created by organs like the skin. Changes to the voltage in and around the cells change their behaviour in the same ways physical and chemical stimuli can. For example, when the skin is ruptured, the potential build across it is shorted at the wound site which creates a current flowing into the wound and up and back through the uppermost layer. This current creates an electric field across the cells which has been shown to cause skin cells to either move with or against the direction of the field depending on their type [1].
Other examples include the differentiation of neural progenitor cells into neurons for regeneration of neural tissue [2]. Stimulating a broken nerve into better regrowth [3]. Promoting osteogenesis (the formation of bone) [4]. Even ranging to some applications in cancer treatment by modulating the immune response [5].
There is much research to both the optimal way to stimulate and the optimal stimulation parameters; which is something that can change from one type of application to the next. Research on this can be done either in vitro by seeding cells in a well and applying an electric field over those cells or in vivo by implanting electrodes on living animal models. Both methods require time and space to experiment. Even though in vitro has the advantage that not a lot of space is needed for the cells to live, the setup for the stimulation is often large, expensive and/or cumbersome. In addition, prolonged stimulation with contact electrodes can lead to harmful chemical products created through faradaic reactions. This in turn can damage the cells and influence the results of the experiment.
Due to the need for many parallel experiments to find optimal stimulation parameters, devices are made that can independently stimulate small pockets of cells simultaneously to streamline experimentation. It is this part of the field that this paper aims to improve on. In this paper, a new design for a device capable of stimulating multiple wells of cells is proposed. It should be readily usable by biologists doing the experiments and it should maintain charge balance to reduce or almost eliminate harmful chemical interactions between the device and the cells. This leads to the overall goal of this paper:

How many independent groups of cells can be electrically stimulated with different stimulation parameters with a device that has the overall shape factor of a well plate, while preventing harmful chemical interactions between the device and the cells?

1.1 Structure of the report

First, some fundamental parts of the field are explained like stimulation methods, electrode types, and concepts like conductivity, voltage, current and electric field. This is followed in the state of the art in this field. This includes the type of devices used for research and their problems, as well as the current view of optimal stimulation parameters and the ranges in which research is being done.
With this information in mind, a system level analysis of what the device should be able to do is provided. Followed by an in-depth view of the design itself.
Lastly, the results of simulations and physical measurements are shown in chapter 4 followed by a discussion on the limitations of the design and further research suggestions.

2 Fundamentals and state of the art

The field of electric stimulation of cells is a broad one and such, there are many different experiments happening with a wide range of electric and physical parameters. The device this paper presents aims to make these experiments easier to perform and therefore should be able to emulate all different electric parameters used in the current state of the art. While there lacks a general consensus on what exactly to report about the experiment and how, almost every paper tries to convey in some way the intensity of the stimulation and the frequency and length of the pulses as well as the time stimulation was applied. So at least those parameters can be summarized. The problem with intensity, however, is that it is not always given in electric field strength. More often than not, it is given as a current, or a voltage. In the case of the current, the actual electric field the cells experience depends on how much the current spreads out through the media or the tissue. In the case of the voltage, it depends on the distance between the electrodes and the voltage buildup on the electrodes themselves.
This chapter aims to give the required background information to understand the topics discussed in this work. This includes fundamental electrical engineering concepts like conductivity, voltage, current and the electric field. This is followed by more application specific information surrounding the different methods of stimulation and the electrodes that are used for these purposes. Then, the state of the art is described by summarizing the most common ranges of electric stimulation parameters as well as the different electrical designs that are used to achieve those.

2.1 Electric field

Electronics is often thought of in a lumped element view. Meaning that there are discrete elements in the system like a voltage source and resistors. When applicable, this allows for the use of Ohm's law, $V = IR$, to quickly model the different voltages (V) and currents (I) in a circuit with resistive elements (R). This model, however, does not hold when all circuit elements start to meld together without well defined borders. In that case, it's more useful to start looking at a small portion of space and what is happening there instead of looking at the difference between two distant points like with voltage. The gradient of the voltage in an infinitesimally small region of space is called the electric field. It points from positive charges to negative charges, and its units are Volts per meter. When two plates with a potential difference of 1 volt are separated by 1 meter of homogenous space, the electric field in every spot in that space is equal to 1 V/m.
With this in mind, an extension of Ohm's law is: $J = \sigma E$ with J being current density, σ being the conductivity of the material and E being the electric field. The inverse of conductivity is called resistivity and is usually denoted with the Greek letter ρ.
Using Ohm's law, to get an electric field in a specific spot, one can either apply a voltage over a specific distance or control the current density in the specific spot of interest. Both methods have their up- and downsides due to the circuits needed to control those values.

2.2 Stimulation methods

An important distinction needs to be made about electric current. The definition of current is the movement of charge. In electronics, the charge carriers that are moving are electrons. However, the main charge carriers in the body and culture fluid are anions and cations. Those are positive and

negatively charged atoms or molecules that are free to move around in the fluid. Currents and voltages whose charge carriers are ions are called ionics instead of electronics. For an electronic circuit to create a current and therefore an electric field in the fluid, a conversion between the electronic and ionic domain needs to be made. This can be done in three main ways which are illustrated in Figure 1.

The first way is to inductively induce an electric field by applying a changing magnetic field to the target. This has the great advantage that there is no physical contact between the electronics and the cells or the media which prevents the circuit from unintentionally interfering with the experiment. A major downside is that to create a changing magnetic field, you need a changing current. So while going from zero amperes of current to some higher current creates the desired electric field, there is a limit to how high the current can go. Often by how much energy the stimulation device can take before either the energy source runs out or the device burns down. This means that DC stimulation is not available with this technique.

The second method is to have two large conductive plates on either side of the culture dish. By applying a voltage to the two plates, an electric field is created between them. However, since the electric field strength is inversely proportional to the permittivity of the material, a lot of the electric field that would normally be equal along the distance is focussed in the gaps of air between the plate and the media since the permittivity of air is much lower than that of culture media [6]. Even when eliminating the airgap and placing the plate against the container, the permittivity of the container will still dominate. This, however, does not mean that no electric field is present in the media. Some, although relatively little, fraction of the field is still present in the media and so to have a noticeable field there, the solution is to have a very high voltage on the plates. This technique allows for DC stimulation at the cost of high voltage. And while in vitro, the high voltage can be overlooked as an issue, in vivo, the high voltage can be seen as a potential health risk.

The last method is to have direct contact between the electronics and the media via electrodes. These electrodes either form a capacitive interface between the fluid and the electrode allowing current to flow or they allow current to flow through electrochemical reactions. In the latter case, electrons from the electronics are taken or given in the chemical reaction allowing them to move into or out of the electrode and continue as current. The chemical reactions caused by these electrodes are often harmful either by being cytotoxic themselves or by raising or lowering the pH of the media. Low frequency stimulation is possible using this technique until the voltage on the electrodes become too high and harmful chemical reactions start to occur. However, in contrast to the other two methods, there is no need for high voltages or currents to get a noticeable electric field in the media. The complexity in this method rises from the need to keep the voltage across the electrode below the threshold for harmful chemical reactions.

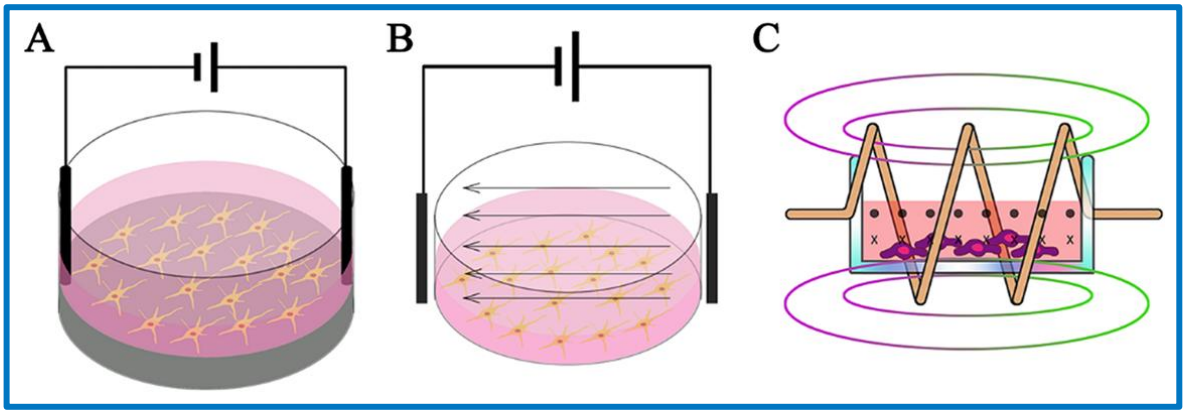

Figure 1: Three different methods for imposing an electric field over cells. From left to right: direct (A), capacitive (B) and inductive (C). The figure is taken from a review on electric stimulation [14].

2.3 Electrodes

Electrodes are used to convert electronic signals to ionic signals. The electrode interface is the place that this happens and has the electrode material on one side, and the solution on the other side. A signal can be passed through this interface in two ways. It can happen by electrochemical reactions which occur when the interface voltage exceeds the electrochemical threshold, or by electrostatic interactions between the electrons on one side of the interface and the ions on the other side of the interface. These processes are called faradaic and capacitive or non-faradaic respectively. Electrodes that only transfer charge through the capacitive process are called ideal polarizable electrodes while electrodes that only transfer charge through the faradaic process are called ideal non-polarizable electrodes.

Faradaic reactions are often a negative side effect of stimulation since the electrochemical species created through the reactions can, depending on the reaction, be cytotoxic [7]. However, even chemically inert elements like gold can have faradaic charge transfer at sufficiently high interface voltages through hydrogen and oxygen evolution. When the voltage increases beyond a certain threshold, the water in the solution reacts with the electrons provided or taken at the electrodes to create hydrogen and oxygen or other molecules like H_2O_2 [8].

Since electrodes have these two pathways of charge, it is often sufficient to model them with a capacitor in parallel with either a resistor or another electrical element to model the faradaic reactions. This model is called either an RC-model or Randal's circuit and is showed in Figure 2. Here, R_s is the resistance that models the wire resistance, as well as the solution resistance and any other parasitic series resistances with the electrode. C_{dl} models the double layer capacitance, which is the ratio of charge to voltage on the electrode interface. This capacitance is the non-faradaic process of charge flow which happens due to charge buildup on the electrode which repels like charges and attracts opposite charges in the solution. Creating something that behaves as a capacitor. R_{ct} models the charge transfer due to faradaic reactions. It is not uncommon to have a voltage threshold in series with this resistance to model the needed voltage before current flows, or to use other electric elements to model the non-linearities of electrochemical reactions. However, for the basic understanding of electrode workings, a resistor is enough.

There is only so much charge that can be injected into the electrode before the voltage rises too high. The charge needed to get the voltage high enough to start chemical reactions with water is called the charge injection limit and is measured in coulombs for a specific size electrode. However, when discussing different materials and electrode fabrication methods, the sizes of the electrodes are not

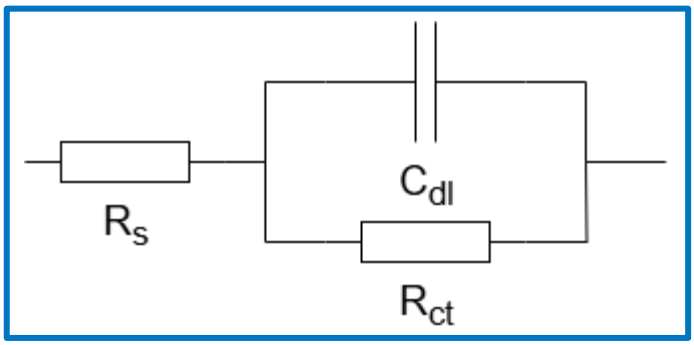

Figure 2: Randles circuit. R_{ct} models the faradaic charge transfer of the electrode. C_{dl} is the double layer capacitance and models the non-faradaic charge transfer. R_s encapsulates any series resistances.

always the same. Therefore, it is also common to measure the charge injection limit in coulombs per square meter, or a differently scaled unit for charge per square area.
Different materials have different electrochemical reactions and different charge injection limits in addition to different interface impedances. The perfect electrode for both stimulation and measuring has zero interface impedance, does not produce harmful chemical products and builds up no voltage on the interface irrespective of current. Since this electrode does not exist, a trade-off needs to be made in terms of these attributes. For stimulation, electrochemical reactions are a bad thing but other than needing more voltage headroom in the stimulation circuitry, voltage/charge buildup on the interface is not a problem. Neither is the interface impedance within reason since the voltage drop over this interface can be compensated by stimulating with a higher voltage. The charge buildup only becomes a problem when the voltage becomes too high, which is why stimulation electrodes are often optimized for high charge injection limits. In contrast, measurement electrodes should have no voltage buildup on the interface since it is impossible to distinguish the voltage buildup from the measurement without additional knowledge. This is why measurement electrodes often use non-polarizable electrodes such that charge transfer happens through electrochemical processes. This does mean that harmful chemicals are added to the solution but since the current in measurements are extremely low, the amount of the chemicals is as well, and safe levels can be maintained.
That being said, a reference electrode does not need to be perfectly non-polarizable to be used as such. The work of Niekerk showed that stainless-steel electrodes could also be used as reference electrodes with tolerable tolerance when compared to Ag/AgCl electrodes [9]. Using materials like stainless-steel can be advantageous since it is more readily available than Ag/AgCl electrodes and could make whatever device that uses them cheaper.
High charge injection limit for stimulation electrodes can be achieved in different ways. One of the ways is to increase the surface area of the electrodes by for example making a mesh of the material, engraving it with grooves, or creating multiple folds where the solution can pass through and between. However, different materials also allow for different charge injection limits. Where metal electrodes can only have charge on the surface of the material, it is possible to create polymeric electrodes where ions can freely move in and out of the material allowing for volumetric capacitance. This means that the amount of charge that the electrode can hold is no longer defined by the area but by the volume. A popular material for volumetric electrodes is PEDOT:PSS which has shown itself to be biocompatible, low in impedance and stable [10], [11], [12].

2.4 Parameters

The stimulation parameters used in experiments differ per cell line and intended goal. Most stimulation done with the goal of wound healing occurs around 50-200 mV/mm at very low frequencies [1], [13], [14], [15], [16]. Trying to mimic or enhance the endogenous electric field created by the skin at a wound without running into the problems caused by direct DC stimulation like electrochemical reactions. Additionally, electric stimulation with the purpose of modulating cell behaviour is mostly done in the same range as for wound healing with similar amplitude and frequency [17]. While stimulation done with the intended purpose of disabling the activity of for example cancer cells is done at frequencies above 50 kHz and amplitudes similar to wound healing and modulating cell behaviour. There are, however, also branches in stimulation with electric fields exceeding 100 V/mm with the result of cell death or electroporation [18]. This branch of research is focused on using electricity in a negative way for cells to specifically target bad cells. Or use electroporation, which normally is bad for cell health, to regulate the uptake of extracellular chemicals while keeping it at a tolerable level for cell viability.

While these are the typical values for research and seem to yield the best results, research is done at amplitudes above and below these limits. In the same review papers cited previously this chapter, amplitudes ranged from zero to 1000 mV/mm with frequencies ranging from DC to 500 kHz. Although such high frequencies are not common, pulses in the microsecond range are, which requires high frequency control over the signal.

2.5 Devices

To facilitate the research, several devices have been made to increase the control of the electric field over the cells while limiting the side effects of stimulation. Shaner et al. tested multiple channel shapes where the electrodes could be placed in relatively large wells remote from the cells to avoid the side effects [19]. Multiple channel shapes were simulated to create the most uniform electric field while also allowing physical access to do something called a scratch assay. Which is where cells are grown in a layer before scratching part of it to see how fast it grows back. Something done frequently in the in vitro research on wound healing.

Another approach to minimize harmful side effects is to fully characterize the system to know the upper bounds. Which is something that Srirussamee et al. did. They made a stimulator for a well plate with six wells and then modelled not only the electric field but also the electrode performance using simulations. Verifying the results experimentally, showing that already great control over the electric field shape and electrode performance can be achieved without either overly complicated electronics or strangely shaped channels [20].

A great example of a high throughput device is presented in the work of Du et al. where they designed a 96-well plate with simultaneous stimulation of different parameters in different wells [21]. However, the design of the device is glossed over in the paper and rather, the focus is on the results of the biological experiment.

3 Design

The goal of the device is to stimulate a range of different groups of cells while independently changing the amplitude and timing parameters per group. It should do this while being easily usable by the person doing the experiments and by being predictable and accurate in the way it stimulates.
By shaping the device to be compatible with well plates, it can easily be adapted in the process flow of any biology experiment. This creates the first requirement in that the total device should attach to a well plate without obstructing the functioning of the well plate. The shape also dictates the shape of the channels. Every well in the well plate can have a separate stimulation circuit to allow for independent experimentation in every well. The number of wells then dictates the total area available for this circuit.
Precise control of the electric field over the cells include control over the amplitude and timing of the field. The field should also be uniform over all cells in the channel.
Lastly, the device should not harm the cells unintentionally by producing harmful electrochemical byproducts or otherwise. To solve the chemical products from forming, the device will maintain charge balance. Thereby, not allowing the voltage across the electrodes to exceed the threshold for electrochemical reactions to occur.

3.1 Channel shape

The shape of the channel is dictated by three requirements:

- It should fit inside a well of a well plate.
- It should have enough room to allow the cells to migrate, proliferate and be imaged.
- It should shape the electric field in such a way to be uniform over the cells.

One of the many experiments that can be done with electric stimulation of cells is to see how fast they migrate in the presence of an electric field. This preferential migration of cells along or against an electric field is called galvanotaxis or electrotaxis. In which the cells can migrate at up to a hundred micrometres per hour [22], [23], [24], [25], [26], [27]. To properly see this migration, the channel should allow room for the cells to move for a couple of hours. Over the course of a twelve-hour experiment cells can move roughly a millimetre which gives a chosen minimum width/length of one mm.
The shape of the channel can be any arbitrary shape. However, for most shapes, it is difficult to create a uniform electric field. While a rectangular shape is both easy to fabricate and easy to have a uniform electric field. This can be done by having two parallel electrodes on either side of the channel both reaching from the bottom of the channel to the top of the fluid.
To fit the channel into a well of a 48-well plate, it should fit in a circle with a diameter of 10.7 mm and a height of 17 mm.
There are, apart from physical limitations on the channel size, also electrical limitations. To sustain a specific electric field over a specific length, a voltage proportional to the electric field and the length is needed. In addition, a specific current density is required for a specific electric field which can be calculated by dividing the required electric field by the conductivity of the material. Since the total required current then scales with the cross-sectional area of the channel, it cannot be made infinitely large. While this need not be a problem, it can become one depending on other trade-offs in the circuit design.
In summary, the channel needs to be rectangular with an area of at least 1 mm x 1 mm to accommodate the cell movement and maximally 10.7 mm from the centre in any direction to fit in the well. Finally, the height needs to be at least 5 mm to accommodate cell culture media and at most 17 mm to fit in the

well. However, these upper requirements are only relevant if the channel is made inside a well. Any type of channel could be stimulated which puts the upper limits on the circuit design. The length is set by the maximum voltage of the supply and the maximum desired electric field. While the width and height limitations are set by the current driving capabilities of the stimulator.

3.2 Current generator

Assuming that the design includes some user interface circuitry which allows the user to turn some waveform configuration into an electrical signal. There should exist a piece of circuitry that converts this electrical signal into a current that gets sent to the electrodes. This current should be as stable as possible ignoring all external influences like electrode voltage and channel impedance.
While it is possible to have the configuration circuitry output some current as a signal, it is easier to share a fixed voltage at several points than it is to share a fixed current at several points. Therefore, the circuit needs to behave in some transconducting manner. Turning the configuration voltage into the current it represents.
The circuit should be capable of creating electric fields up to 1000 mV/mm. This, together with a conservative estimate of the transconductance of cell culture media being 1 S/m [28] gives a current density requirement of up to 1 mA/mm^2. Taking into account a rough maximal cross sectional area of the channel as presented in chapter 3.1 with a fluid height of half the well height gives 10.7 * 8 = 85.6 mm^2 which gives a maximum current of roughly 86 mA. The frequency range this device should be able to stimulate is from zero to about 500 kHz, but higher values are better to get shorter pulses and sharper control over the signal. Lastly, the theoretically required voltage headroom is equal to 1000 mV/mm multiplied with the maximum length of the channel which would be roughly 10 mm. This results in an estimate for required voltage headroom of 10 V. To this, some margin should be added to be used for the transconductance amplifier and to allow voltage to build up on the electrodes without influencing the current.
Both positive and negative stimulation needs to be appliable which means that current needs to flow both ways. There are two ways to achieve this. The circuit can either use two supplies, one negative and one positive, to both push and pull current in either direction. Alternatively, the circuit can flip the load around such that the direction of current is reversed. This has the benefit that only one supply is needed at the cost of circuit complexity. Another advantage to the single supply solution is that the control part of the circuitry can operate on the low side of the load with a translating component that can handle the high voltage and current of stimulation. In discrete components, it's not uncommon to trade voltage and current capabilities for bandwidth so this is greatly beneficial.

A typical transconductance amplifier consisting of an amplifier, a mosfet, and a resistor was chosen for this device. The polarity of stimulation is determined by an h-bridge on the high side of the amplifier. The circuit diagram can be seen in Figure 3. This configuration has the main advantage that no dual supply is needed. Additionally, the input of this circuit can be at 5 V or 3.3 V with the amplifier at the same voltage level while the mosfet translates the output of the opamp into a big current for the electrodes. This means that the opamp can be chosen purely for the bandwidth performance while almost any discrete mosfet with a high enough voltage and current rating works. The more difficult to find components of this circuit are the h-bridge elements which can be either made using discrete mosfets, which would require bootstrap circuitry to drive, or analog switches with a high enough voltage and current rating. The analogue switches where the better choice in this case since they are smaller and cheaper. However, if more current or voltage is required, the analogue switch solution runs out of components to choose from.

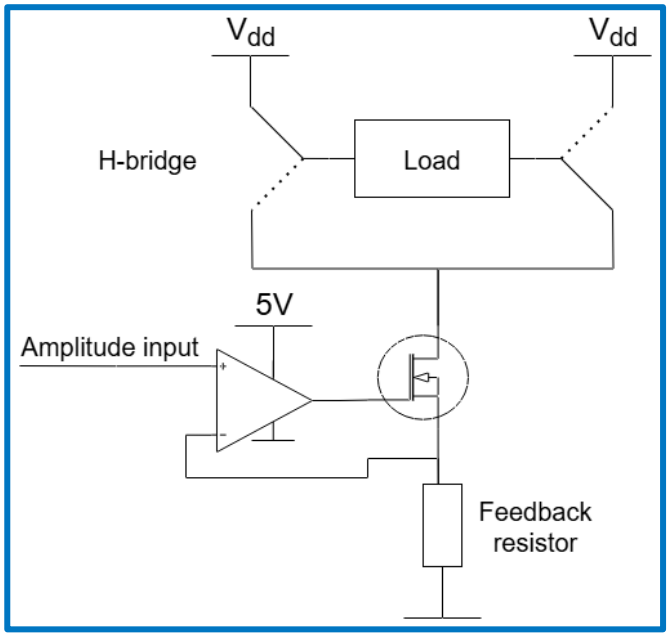

Figure 3: Circuit diagram of a transconductance amplifier in conjunction with an H-bridge.

3.3 Configuration circuitry

The configuration circuitry should turn whatever electric stimulation configuration the user has in mind into electronic signals that the output stage can work with. The information required for the output stage to create the stimulation is the amplitude for both the positive and negative phase, and binary information regarding polarity and the on-off state.

3.3.1 Amplitude

The amplitude can be created by any circuit that has a variable voltage output. The first thing to come to mind would be a voltage divider with perhaps a potentiometer for user input. However, potentiometers with a reasonable price tag and size have a tolerance of at least 5%. Which means that the exact same amplitude setting on one channel can differ from the next by 10% already due to the component choice alone. Alternatively, there exist resistors with a high tolerance of 0.1% or lower. Creating a voltage divider with these resistors can create very accurate voltages that don't differ much between channels. The obstacle then is the user input side. The user should be able to easily change the resistor value in the divider to create a different voltage and thus a different amplitude configuration. This can be solved by using pin headers and jumpers to physically connect the middle of the resistive divider to a resistor on both sides. Options can be added by allowing the top and bottom resistors to each be chosen out of a series connection of N resistors. Excluding shorts and using twice N resistors (one bank for the top and one for the bottom), this concept gives $(2^N - 1)^2$ options. For five resistors on the bottom and five on the top (N=5), this gives 961 configurations. The last problem to solve is that the configurations should scale exponentially since the difference of 1mV/mm is much more interesting

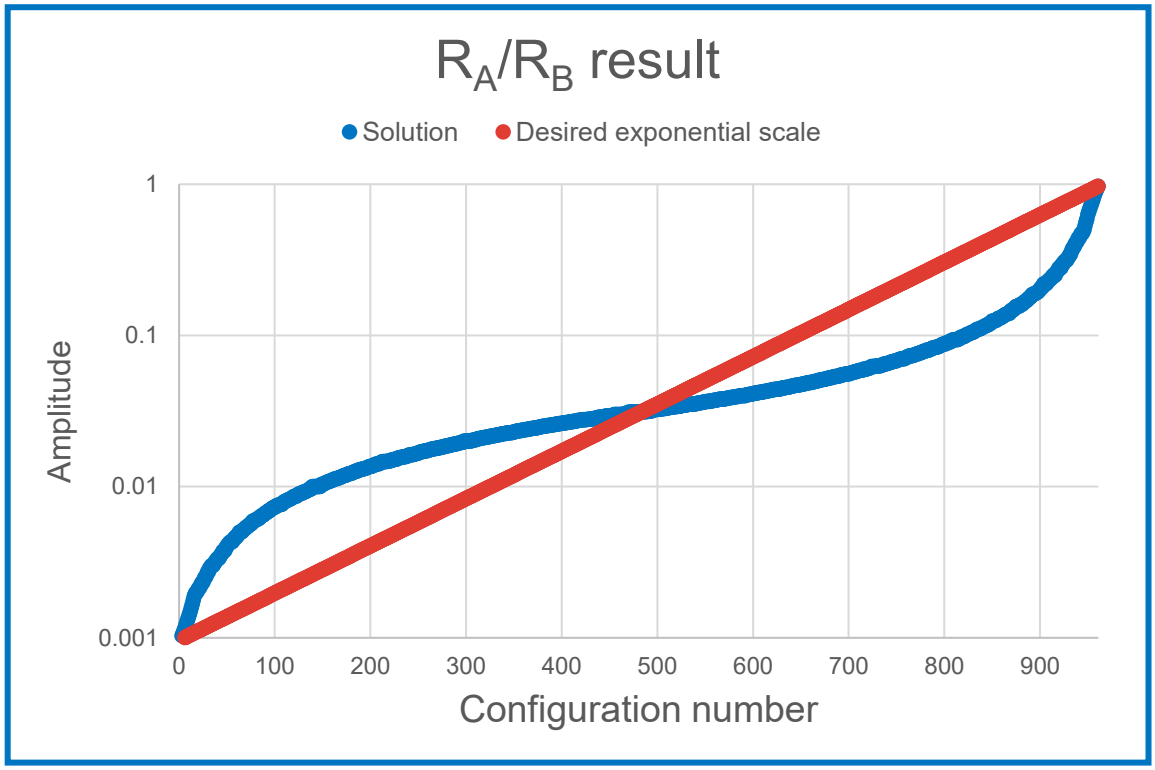

Figure 4: A plot of a sorted list of two 5-bit numbers divided by each other on an exponential scale. The first number is any series connection of [16k, 8k, 4.02k, 2k, 1k] ohms and the second number is any series connection of [500, 250, 130, 60.4, 30] ohms. The amplitude is given in a unitless ratio of the two numbers and the configuration number is the position in the ordered list. In total, there are 961 combinations because zero divided by zero would cause the PCB to burn.

at 5 mV/mm than at 1000 mV/mm. Building on the resistive divider principle, if it is possible to first create a current through one of the resistor banks independently from the other resistor bank, and then convert that current into a voltage on the second bank, an R_A/R_B configuration can be made. Where R_A and R_B are the chosen resistors. This is not quite exponential, but it does fit an exponential curve relatively well near the centre. With 961 configurations, almost three orders of magnitude can be covered and roughly two of those are close to exponential as can be seen in Figure 4.

The selection of resistor values is done by placing all five resistors in series and placing a header in parallel to each resistor. Thereby giving the user the option to short any or all of the five resistors.
The voltage to current conversion is done with negative feedback, an operational amplifier and a mosfet. A voltage reference is used to keep the voltage above the mosfet, and therefore the voltage over the top resistor bank constant through the negative feedback. The resulting current is led into the bottom resistor bank which produces the output voltage of the circuit. This entire circuit is illustrated in Figure 5.

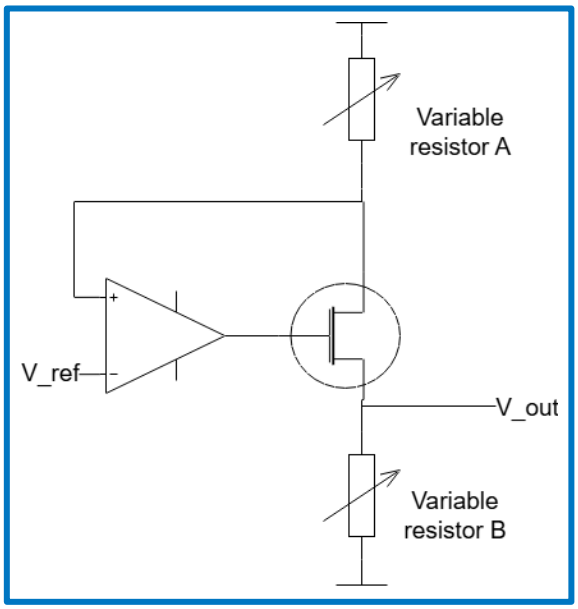

Figure 5: A/B voltage divider using negative feedback to create the transfer relationship.

3.3.2 Timing

The timing circuitry should create three distinct waveforms: the waveform for the anodic part of stimulation, for the cathodic part of stimulation and for when the stimulation should switch from anodic to cathodic. All these waveforms consist of an on-period and off-period with specified lengths. So, to create any of the three waveforms, a circuit is needed that outputs a high voltage for a specified time before turning off, to then turn on again after a different amount of time has passed. The flipping of the output state can be done using a flip-flop which turns on at the rising flank of one clock signal and turns off on the flank of another clock signal. In that case, to create the desired output signal, two clock signals should be created with flanks at the specified times. Assuming some core frequency, a clock signal with a specified period can be created by dividing the clock signal by two an arbitrary number of times. There exist logic chips that do this, either dividing the signal frequency by two or by some other power of two. This principle gives access to any slower multiple of two of the starting frequency. If more control over the time is required, a counting chip can be cascaded. This chip takes in a clock signal and counts to some configured number before giving a flank signal. This logic block is illustrated in Figure 6 and is repeated once with the counter to determine the on time and once without the counter for the off time. This means that the duty cycle of the output can be tuned in steps of 0.4% or smaller while the

period of the output is always a multiple of two of the seed frequency. Omitting the counter from the second block was done to safe space.

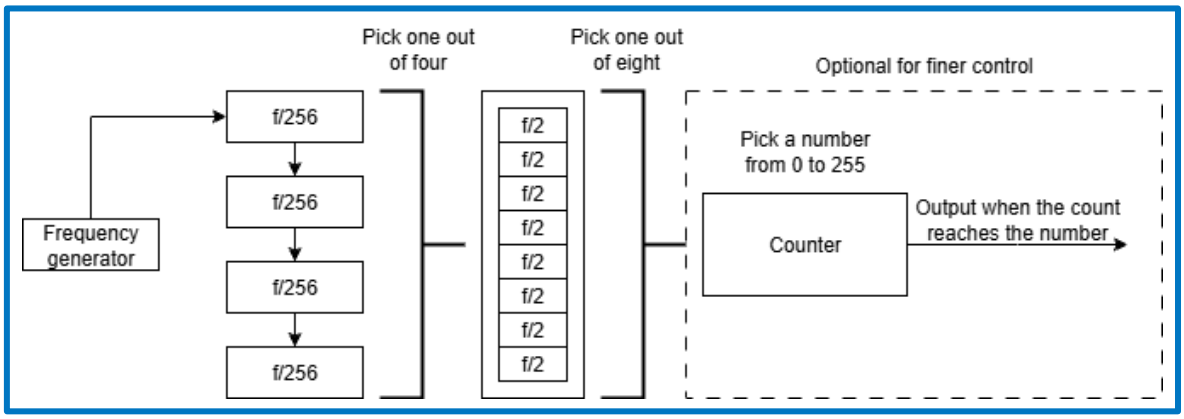

Figure 6: Illustration of how any seed frequency can either be turned in a slower multiple of two or any lower multiple of two multiplied by some count.

3.3.3 User input

Both the amplitude and timing circuitries require user input to be configured. The amplitude circuitry required the user to somehow short resistors and the timing circuitry required a binary input for the count and the ability to choose which of the clock signals gets passed on to the next section. The way this design does this is by using pin headers and jumpers. They are metal pins that point out of the PCB that can be connected using the jumpers. This allows the user to physically connect two traces together and thereby choose clock signals and short resistors. The digital input is done using the same principle but using an extra pullup resistor and allowing the pin header to short the input to ground.
An alternative to this method is to use multiplexers for the trace connections and shift registers for the user input. Both chips can be controlled using a microcontroller which can get the user input through some screen and button combination of input or through a cable from a computer. This has the advantage of being more intuitive to use and does not require small jumpers. However, it does require the microcontroller to be programmed which would add another step in the assembly process.

3.4 Charge balance

Charge balance of the electrodes is achieved by making sure that at the end of stimulation, there is little to no charge left at both electrodes. This is done to prevent the voltage on the electrode interface to exceed electrochemical thresholds. This is usually done by either making sure the positive part of the stimulation inserts the same amount of charge the negative side removes or by measuring the excess charge and removing it in a separate manner.
To give as much freedom in stimulation as possible, this work proposes that the charge on the electrode is measured and that stimulation is stopped during the negative part when the charge reaches the zero crossing. This gives the researcher control over how the electrode is discharged.
This is done by adding a third non-polarizable electrode as close to the anodic working electrode as possible. This electrode measures the voltage on the working electrode using a comparator chip and when the voltage becomes zero, the comparator outputs a signal that shuts of the stimulation. This circuit is shown in Figure 7 where the stimulation is in the negative phase. The dotted lines indicate the connections for the positive phase.

Choosing the right comparator involves the bias current, reaction time and voltage rating. The lower the bias current, the less chemical products are created by the measurement electrode. The reaction time should also be as fast as possible to allow for fast stimulation time. The fastest this design aims to stimulate is with two microsecond periods, meaning that the comparator should at least turn of stimulation faster than one microsecond. If it reacts slower than the negative phase lasts, it doesn't have any effect since it can't turn off the stimulation if it's already off. Lastly the comparator will be exposed to the full stimulation voltage meaning it should be voltage rated accordingly.

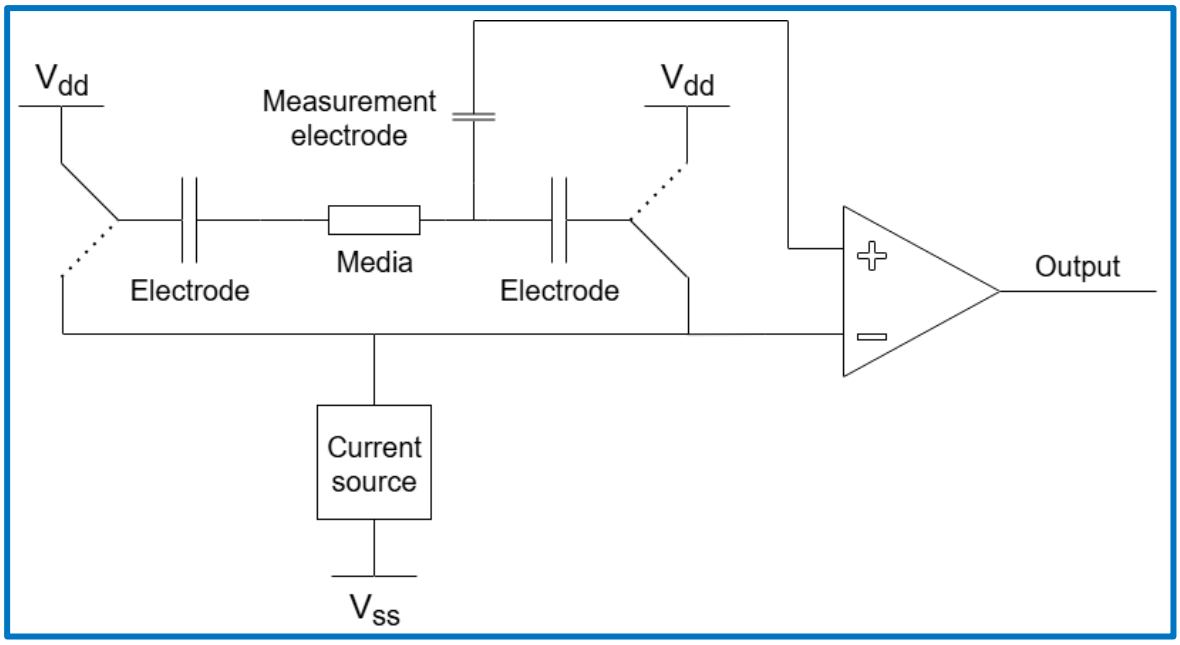

Figure 7: Circuit concept of a comparator measuring the charge on one of the electrodes. The two working electrodes are polarizable electrodes while the measurement electrode is non-polarizable. Allowing the comparator to measure the voltage, and thus the charge, on one of the electrodes during the negative phase of stimulation. The dotted lines indicate the connection during the positive phase.

3.5 Electrodes

There are three electrodes in the system. Two of them allow the stimulation current to flow and therefore handle a relatively big current. This means that they should not produce any cytotoxic chemicals due to the stimulation. This is why PEDOT:PSS was chosen as the material. It boasts a high volumetric capacitance allowing to remain in the polarizable regime of DC stimulation for longer than materials like platinum or gold. It is also shown to be biocompatible. The fabrication of the PEDOT:PSS electrodes used in this work is shown in Figure 8 and follows the protocol designed by Savva et al [29].

A glass waver with an indium tin oxide (ITO) coating was cut to size (55 mm x 5 mm) using a glass cutter. PEDOT:PSS was prepared using 5 vol% ethylene glycol (EG), 1 wt% 3-glycidoxypropyltrimethoxysilane (GOPS) and 0.002 vol% dodecyl benzene sulfonic acid (DBSA). Then PEDOT:PSS was dropcasted on roughly one quarter of the strip. Followed by a short annealing step of one minute of 90 C° and a long annealing step of at 125 C° for 45 minutes. Finally, one quarter was isolated with Kapton tape, and one quarter was taped with copper tape to create a landing pad for the wire to connect it to the electronics.

The stainless-steel electrodes were cut from a 316-grade stainless-steel mesh (Woven Wire Mesh, 325 mesh, Inoxia) and rolled to achieve a compact electrode. Afterwards, copper tape was taped and soldered to the mesh to provide a landing pad for wires.

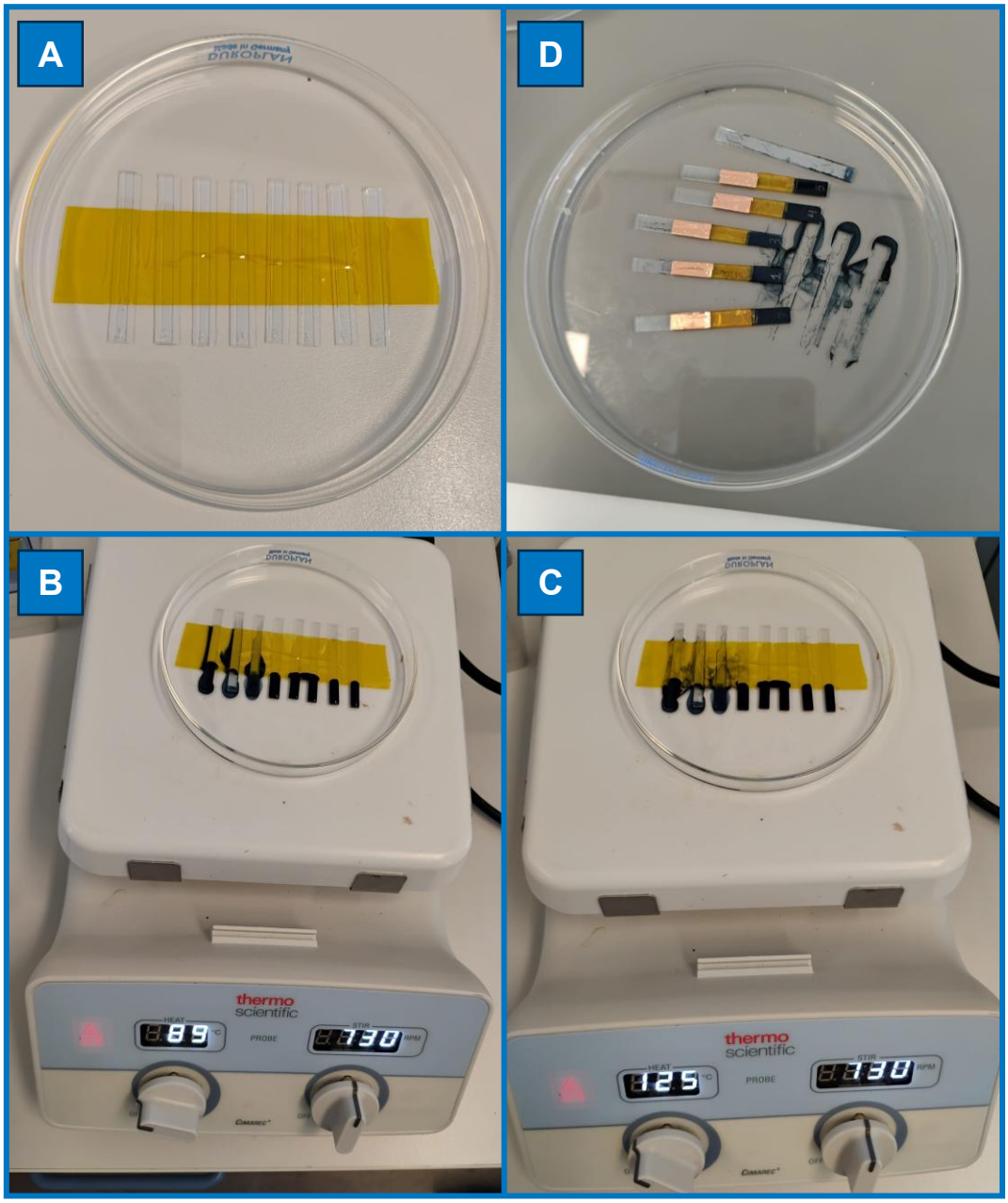

Figure 8: Fabrication process of PEDOT:PSS electrodes. Going counterclockwise: the glass-ITO substrates are cut to size (A), PEDOT:PSS is dropcasted on roughly one quarter of the slides and preheated at 90 C° (B); The slides are baked at 125 C° to remove any moisture (C); the slides are taped using kapton tape for isolation and copper tape as a solder pad for wires (D).

3.6 Component choice and PCB

The components were chosen to be available at the time of production at Farnell. The only components not bought at Farnell are the pin headers and jumpers. Those were bought at AliExpress. The underlying tables outlines what components are chosen per section of the device, what their most important specifications are and how much it costs. In summary, there are three main subcircuits that are worth counting. There is the circuit that creates the timing sequence for a column as shown in Table 1. It costs about €14.82 in components, and you need at least one of them for stimulation. The same goes for the configuration circuit that creates the amplitude. It is shown in Table 2 and costs about €4.08 to make in components. For every channel that needs to be stimulated, one output stage is required which is shown in Table 3 and costs about €5.07 to make. Finally, every board needs the auxiliary circuits that distribute power through connectors and create the seed frequency and reference voltage required for the timing and amplitude configuration respectively. It is shown in Table 4 and costs €5.35. So, for a full 48-well plate, you need 48 output stages, 8 timing circuits, 6 amplitude circuits and 1 auxiliary circuit which comes to a total of €391.75.
The PCB was ordered with Eurocircuits and while this work only created a PCB for two columns, a full well plate sized product would cost about €261.48 gross on Eurocircuits. This would bring the total for a 48-well plate stimulation device to €653.23 excluding the time and effort it would cost to fabricate such a device.
The device used in this work was made by hand using a soldering oven and a stencil. The result can be seen in Figure 9. The top image shows the top view; the middle image the bottom view and the bottom image shows the two PCBs stacked on top of each other as they would be when stimulating. The inputs for the configuration circuitry are the pin headers shown in Figure 9B on the left. The slits that can be seen in every image on the output stage PCB (the right PCB) are there to allow the observation of cells without the removal of the PCB.

Table 1: Costs of components for the circuit generating the timing sequence of an entire column.

Part	Amount	Cost (€)	Specification
Capacitor	22	1.760	100 nF (decouple)
Resistor	24	0.144	100 kΩ (pullup)
Pin header 1x3	1	0.179	2.54 mm pitch
Female pin header 1x3	1	0.136	2.54 mm pitch
Pin header 2x3	21	2.904	1.27 mm pitch
Binary Counter (74HC40103PW)	3	1.917	8-bit count, fmax = 15 MHz
8-stage divider (74AHC1G4208GW)	9	2.628	fmax = 125 MHz
Inverter (74AHCT1G14GW,125)	4	0.450	Propagation delay = 6 ns
D-type flip-flop (NC7SZ175P6X)	3	0.510	fmax = 200 MHz
Digital multiplexer (74LVC1G157GW,125)	4	0.395	Propagation delay = 2.2 ns
Binary divider (74HC4520PW)	6	3.811	8 individual 1-bit dividers, fmax = 68 MHz
Total		**14.82**	

Table 2: Cost of components for the circuit that creates the amplitudes used for an entire row.

Part	Amount	Cost (€)	Specification
Capacitor	4	0.320	100 nF (decouple)
Capacitor	2	0.104	1 µF (decouple)
Pin header 1x3	1	0.179	2.54 mm pitch
Female pin header 1x3	1	0.136	2.54 mm pitch
Pin header 2x5	4	0.588	1.27 mm pitch
Opamp (MCP6006)	2	0.472	Used for DC negative feedback
Mosfet (SSM3K72KFS)	2	0.286	Nmos
Resistor	20	1.986	2 per value: 16k, 8k, 4.02k, 2k, 1k, 500, 250, 130, 60.4, 30 ohms 0.1% tolerance
Total		**4.08**	

Table 3:Cost of components for a single output stage.

Part	Amount	Cost (€)	Specification
Capacitor	10	0.8	100 nF (decouple)
Zener diode (MMSZ4678T1G)	1	0.115	Vzener = 1.8 V
Mosfet (SSM3K72KFS)	1	0.143	Nmos
Resistor	1	0.091	10Ω, 0.1% tolerance
Resistor	2	0.019	5.1 kΩ (pullup)
And gate (SN74AHC1G08DCKR)	1	0.059	
Analog multiplexer (74LVC1G3157GW,125)	2	0.395	Switch time = 3 ns
Or gate (NC7SV32P5X)	1	0.126	
Comparator (MIC6270YM5-TR)	1	0.407	Vmax = 36 V Tresponse = 600 µs
Opamp (MCP6496)	1	0.533	GBW = 30 MHz
Analog switch (DG470)	2	2.380	Vmax = 40 V Tswitch = 200 ns Ron = 11 Ω
Total		**5.07**	

Table 4: Cost of components for all auxiliary circuits like the connectors used to transfer power from board to board. Or the crystal oscillator generating the seed frequency. Or finally the reference voltage used by the amplitude configuration circuitry.

Part	Amount	Cost (€)	Specification
Capacitor	4	0.320	100 nF (decouple)
Capacitor	1	0.052	1 µF (decouple)

8-stage divider (74AHC1G4208GW)	3	0.876	fmax = 125 MHz
Bus driver (74LVC1G125GW,125)	1	0.120	Switch time = 2.1 ns
Crystal oscillator (MCSJK-6NC1-1.8432-25-B)	1	1.283	Frequency = 1.8432 kHz Vsupply = 5 V
Voltage reference (LM4041DIM3-1.2/NOPB)	1	1.250	Vref = 1.225 V
Pin header 1x2	2	0.239	2.54 mm pitch
Female pin header 1x2	2	0.272	2.54 mm pitch
Resistor	2	0.016	10 kΩ (pullup)
Slide switch (EG2208A)	1	0.926	
Total		**5.35**	

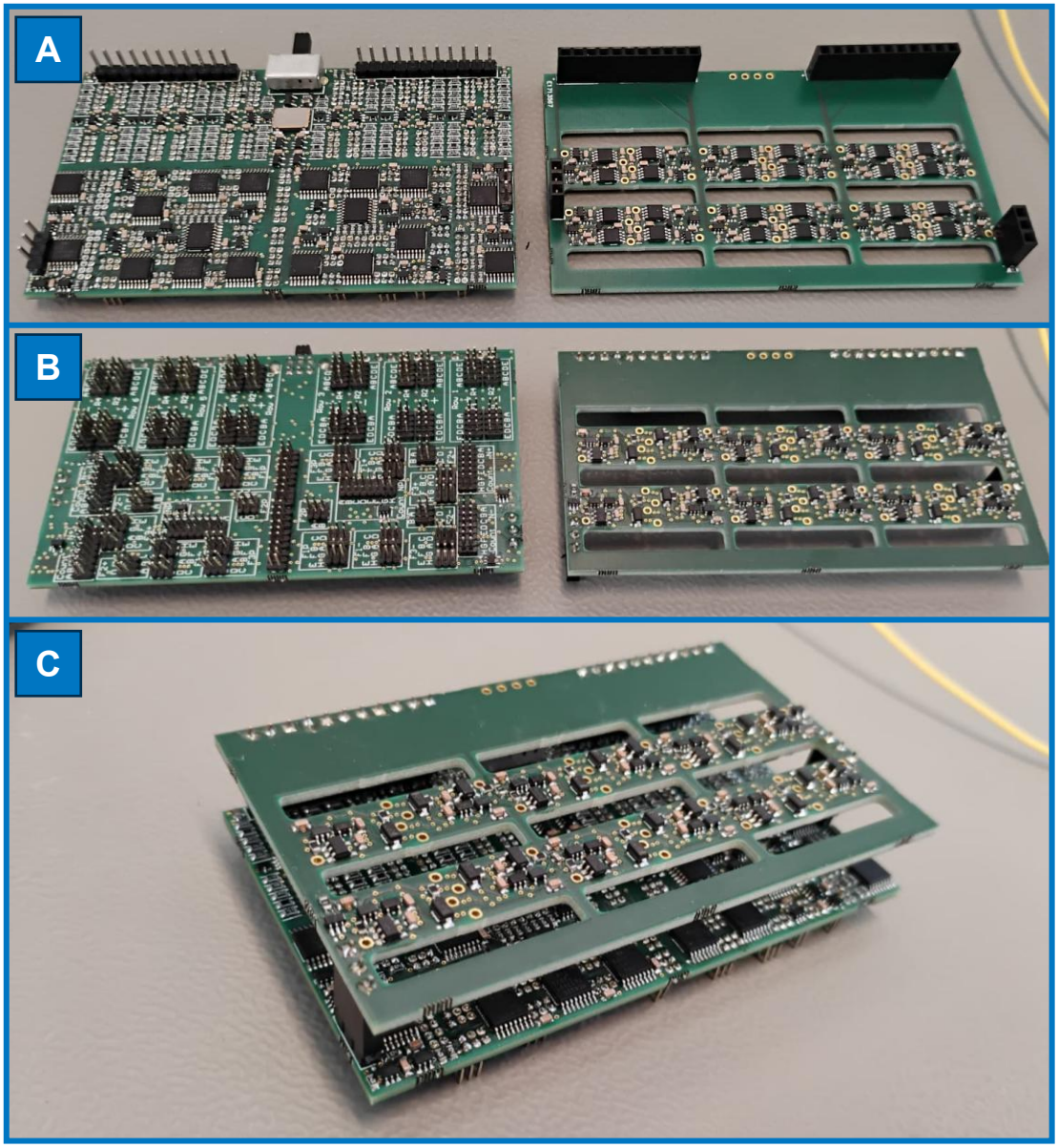

Figure 9: PCB prototype of the stimulator circuit. The top view shown in (A) shows the configuration circuitry on the left and half of the output stage on the right. The other half of the output stage is on the bottom shown on the right in (B). On the left in (B), the input pin headers for the configuration circuit are shown without any jumpers. The bottom image (C) shows the two PCBs stacked on top of each other as they would when stimulating. The slits in the output stage PCB are made to be able to view the cells in wells without having to remove the PCB. They align with the wells, and two wells are above every slit.

4 Verification

To verify that the design is sound, it is tested in LTspice before ordering components. After that was done, extensive testing on breadboard was done to verify the design in the real world. And although those results were riddled with noise, they did prove the potential. Finally, the design was realized on PCB and tested using a C-R-C model for the electrode-media-electrode load.
In addition to circuit simulations, electric field simulations were done to verify the shape of the channel to be correct.

4.1 Circuit simulation

The output stage was tested using LTspice. Not all components match the ones used in the final design, but it still reflects the final workings. The circuit can be seen in Figure 10A and the result of the simulation in Figure 10B. Certain nodes in the circuit are connected to setup circuitry outside the image. State and Polarity are both control nodes that originate from the configuration circuitry. They encode whether to stimulate and in which direction respectively. The line exiting the opamp on the bottom left goes to the amplitude part of the configuration circuitry. In the case of the LTspice simulation, all of these are connected to ideal voltage sources. The node on the bottom right called “Ienable” pulls the amplitude input to ground to prevent stimulation.

The simulation is set up to have two 25 µs pulses of 15 mA and two 25 µs pulses of -20 mA. This can be seen on the green line in Figure 10B. The spikes on the moments of switching are caused by ringing in the model of the ADG633 (the analog switch). The current is cut off when the voltage across nodes D and C (the red line) gets below zero. There is a small delay which is caused by the delay in the comparator. The blue line is the voltage over the other electrode and is chosen to be measured in reverse of the first electrode to not overlap the two signals in the simulation result. Lastly, the cyan line illustrates the output of the comparator to clearly see the moment the comparator detects the zero crossing and stimulation is turned off.

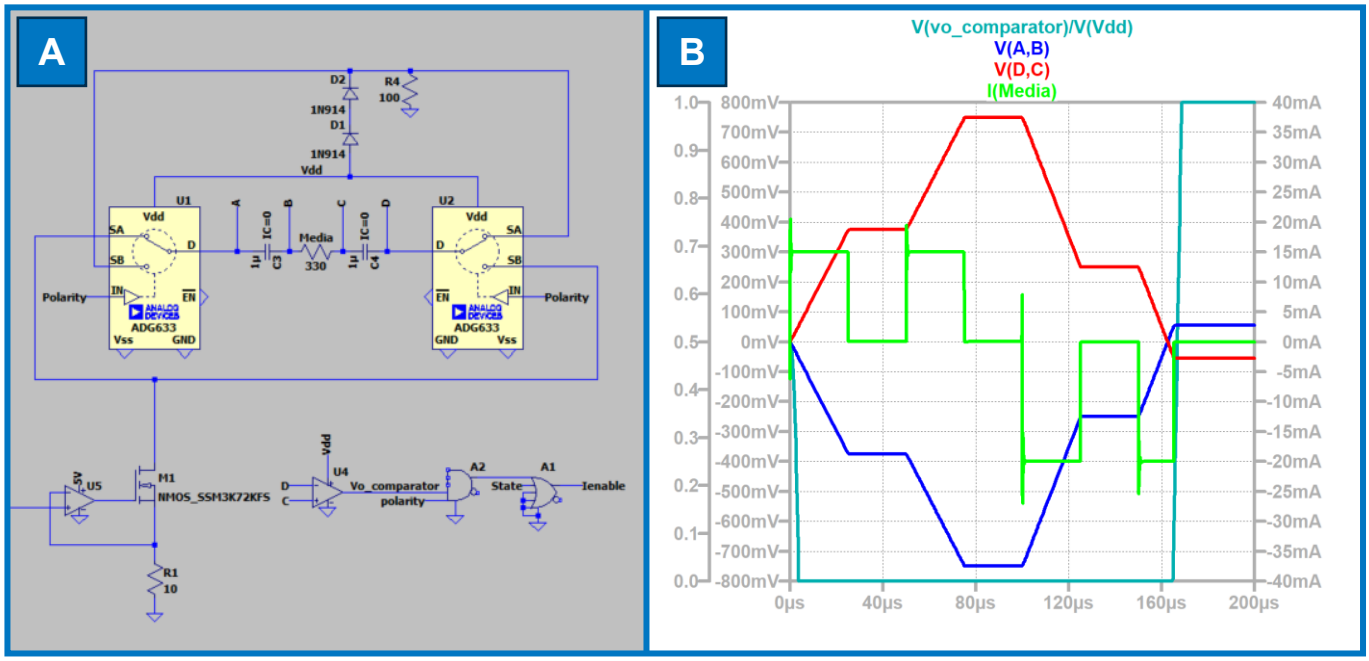

Figure 10: LTspice simulation of the output stage. The circuit is shown on the left (A) with an H-bridge, a transconductance amplifier and a comparator measuring the voltage on one of the electrodes. The result of a simulation is shown on the right (B). The cyan line indicates the comparator logic output which turns off stimulation at a logic high. The blue and red lines are the voltages on the electrodes. They are opposing polarity by choice of reference to visualize them better. The green line represents the current flowing through the media.

4.2 Electric field simulations

Two electrodes separated from each other with some conductive media will have current flow between them. However, this current flow might or might not be uniform through the entire media depending on

the geometry of the channel. To test whether a rectangular channel yields a uniform electric field, a COMSOL simulation was done with two differently sized electrodes. Figure 11 shows the geometry that was used in the simulation. An insulated box surrounds a rectangular channel that is divided into four sections along the vertical axis. The electrodes are placed on the short ends of the channel but vary in height depending on the simulation. In Figure 11A, the two electrodes only cover the bottom two sections while the fluid comes up to the third line, above which is air. This causes the current coming from the electrodes to spread out through the liquid and cause uneven electric fields. A side view is given in Figure 11B.

A more uniform electric field can be achieved if the electrodes cover the entire cross-sectional area of the channel. This means that the electrodes should at least reach to the top of the fluid. This has the effect that the current coming from the electrodes cannot spread out, causing the current density to be the same everywhere in the channel which in turn means a uniform electric field as shown in Figure 11C and D.

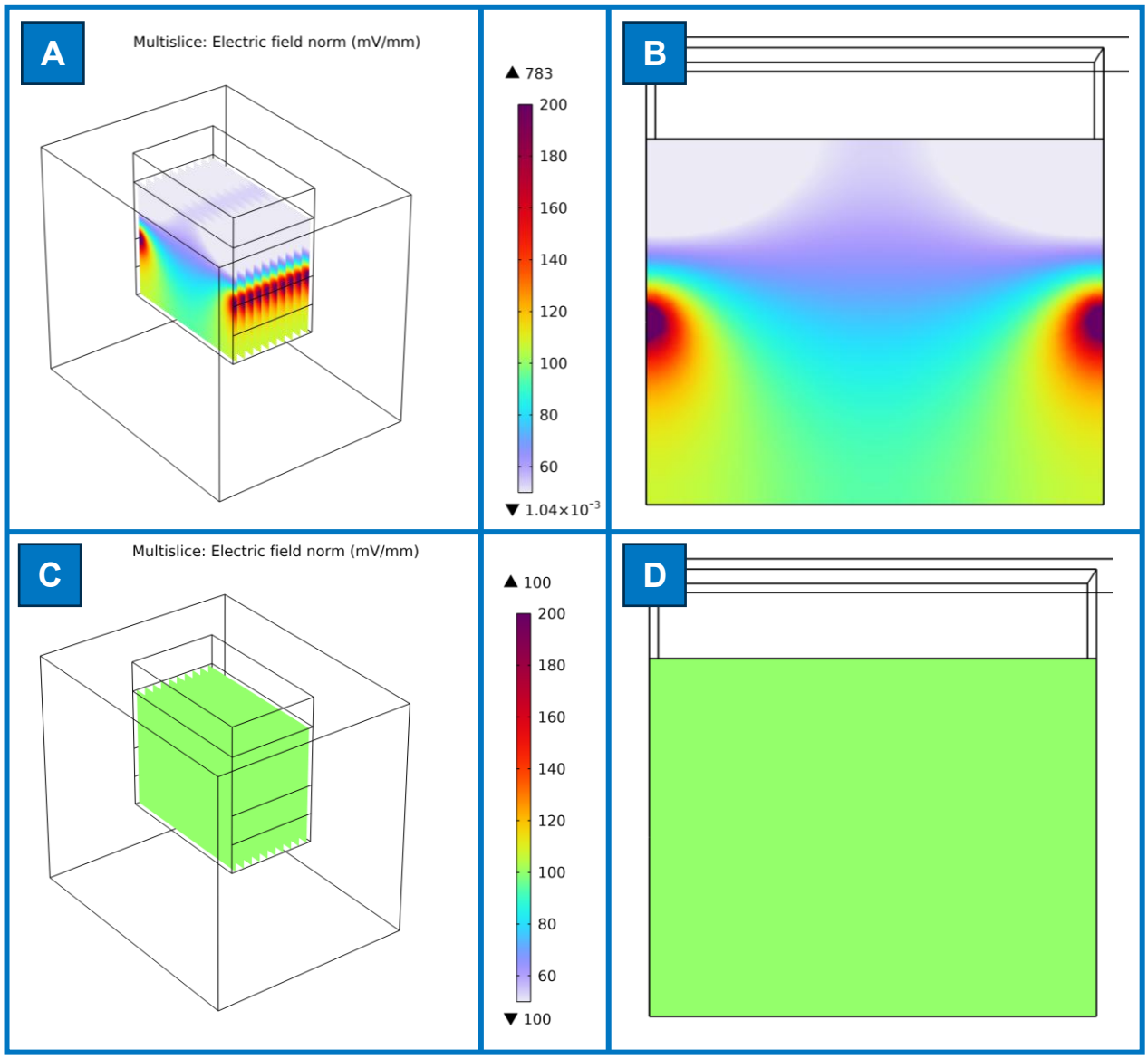

Figure 11: COMSOL simulation of a rectangular channel with two electrodes on either side. The electrodes in the top two images do not reach the top of the fluid (only the bottom two sections) while the two images on the bottom have electrodes that reach the top of the fluid (the bottom three sections).

In this simulation, the channel length, width, height and electrode voltage are chosen to roughly match the channel in the real application, yet the simulation can be scaled arbitrarily without changing the conclusion. The same goes for the conductivity of the media. So long as it is significantly lower than the insulating material of the channel boundary.

4.3 Electrode performance

Two types of electrodes were tested to be used in this work. The PEDOT:PSS electrodes were intended to be used as the working electrodes passing the stimulation current between them. They were fabricated using the process described in chapter 3.5 and tested using cyclic voltammetry (CV) and electrochemical impedance spectroscopy (EIS). A three electrode setup was used to measure the electrodes where PEDOT:PSS was the working electrode and Ag/AgCl was used as a reference electrode. To double check the work of Niekerk [9], one EIS measurement was done using a platinum counter electrode and one measurement was done using the stainless-steel counter electrode. The results of which can be seen in Figure 12. The CV shows almost only capacitive current with only minor increases in current at 0.8 V and -0.8 V. The EIS measurement also shows this capacitive behaviour as the impedance quickly flattens out to roughly 225 Ω which was the contact resistance of the underlying ITO layer. Additionally, both platinum and stainless-steel EIS measurements shown in Figure 12A and Figure 12B are equal for frequencies below one kilohertz. At frequencies above that, the phase increases for the stainless-steel measurements which shows it's not quite ideal, but still usable as a cheap alternative.
To further characterize the stainless-steel electrodes a CV and EIS measurement was made using the stainless-steel electrode as the working electrode, platinum as the counter electrode and Ag/AgCl as the reference electrode. The CV measurement of the stainless-steel electrode seen in Figure 13 shows peaks at voltages lower than those from the PEDOT:PSS measurements. Which hints at the possibility of using stainless-steel as a reference electrode. The EIS measurement shown in Figure 14 show a phase that is not fully capacitive, showing that for the low frequencies, there is some other mechanism for charge transfer than capacitive. This also shows the promise of usability as a reference electrode. Additionally, the phase still remains above zero at frequencies above one kilohertz which explains the phase increase in the EIS measurement with stainless-steel as the counter electrode.

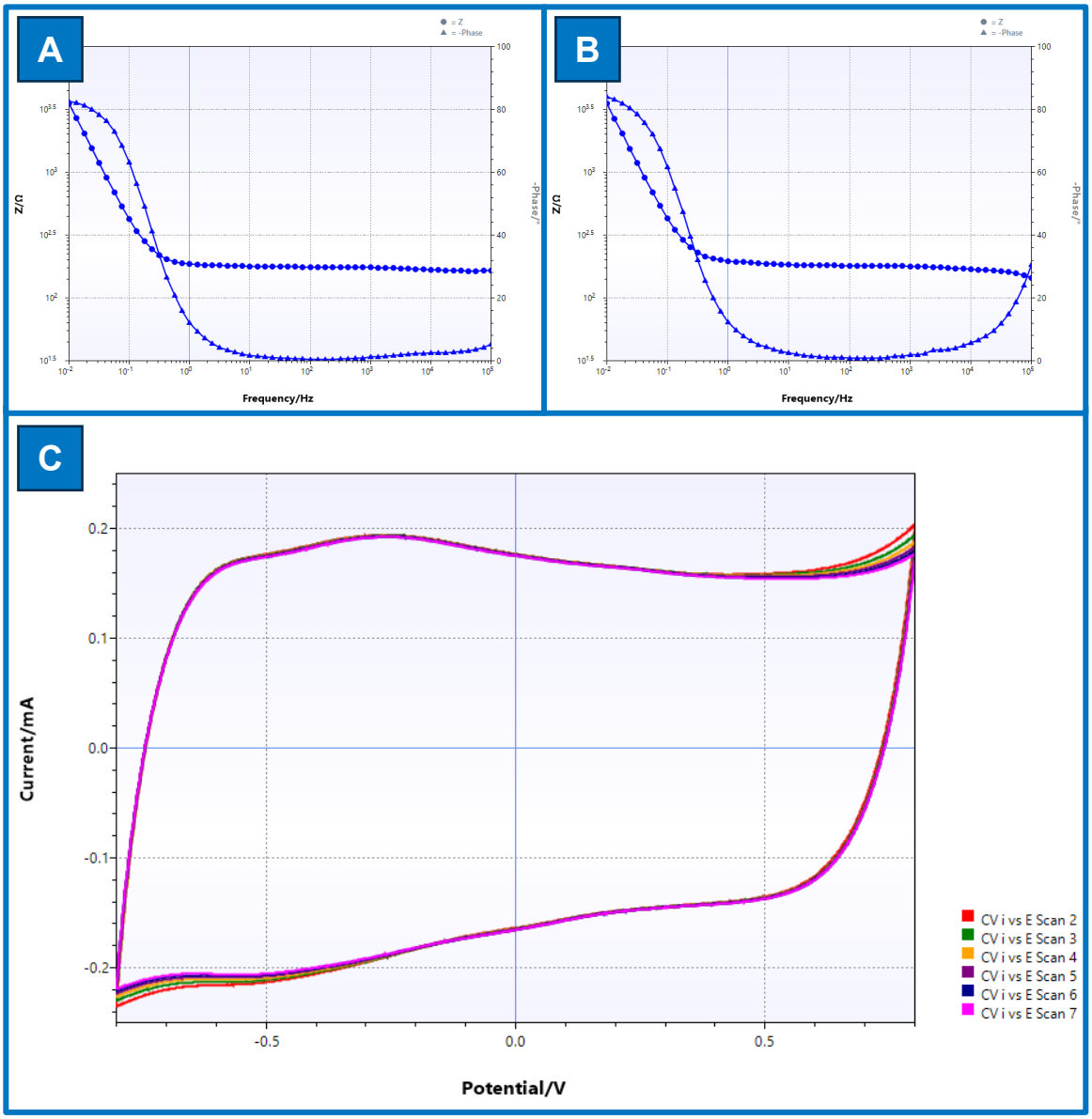

Figure 12: Characterization of PEDOT:PSS electrodes using a three electrode setup. In every setup, PEDOT:PSS was the working electrode and Ag/AgCl was used as a reference electrode. A: EIS measurement using a platinum counter electrode. B: EIS measurement with stainless-steel as the counter electrode. There is no low frequency difference between using the stainless-steel or platinum as the counter electrode. However, at high frequencies (above 1 kHz), the phase does increase with the stainless-steel. C: CV curve of the PEDOT:PSS electrode using platinum as a counter electrode. The measurement was done with seven scans ranging from -0.8 V to 0.8 V at a scan rate of 0.01 V/s.

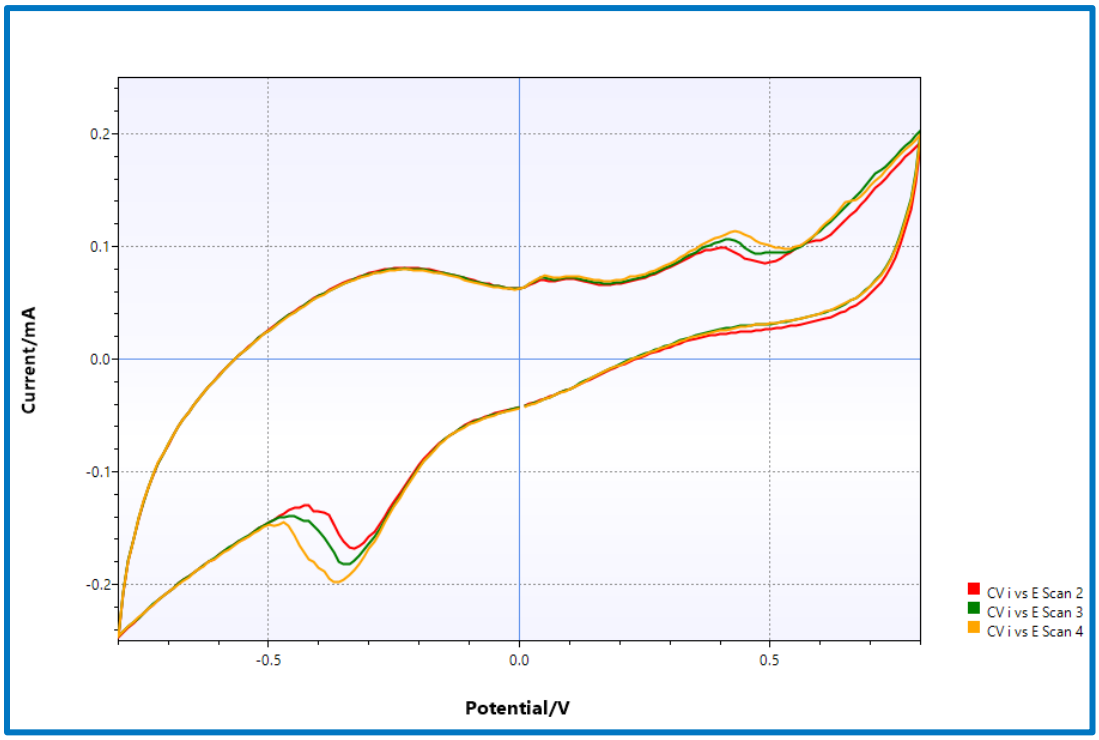

Figure 13: CV curve of a stainless-steel electrode. The measurement was done with three scans ranging from -0.8 V to 0.8 V at a scan rate of 0.01 V/s.

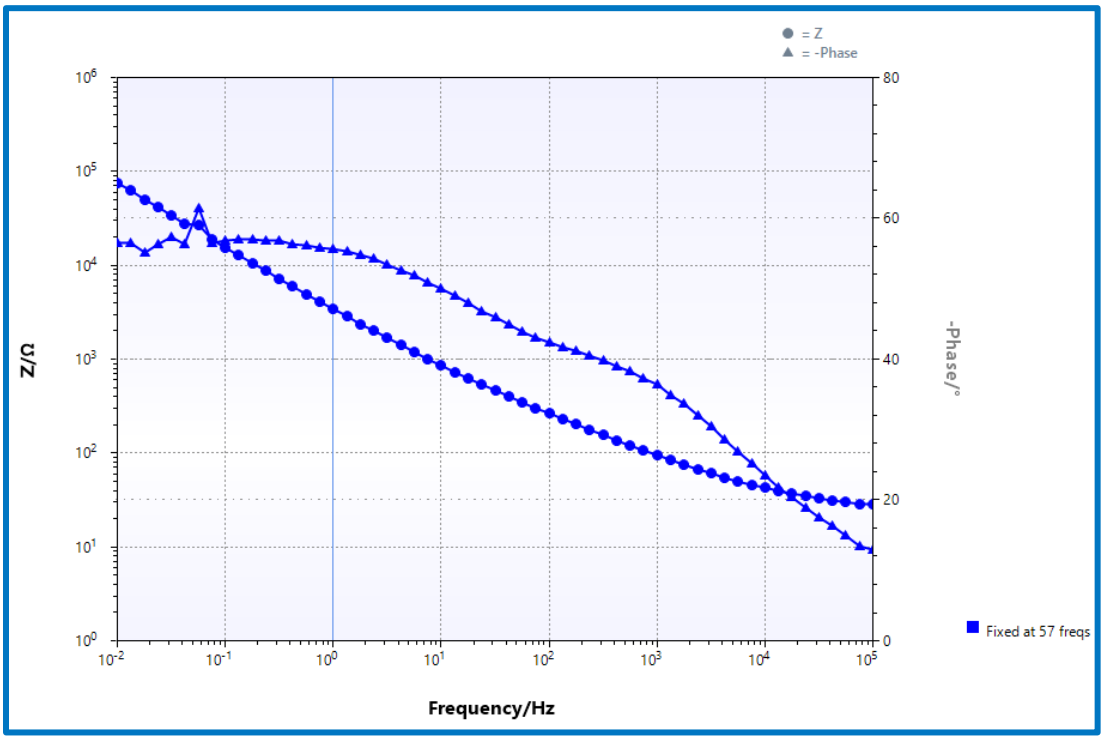

Figure 14: EIS measurement of a stainless-steel electrode. The measurement was done ranging from 0.01 Hz to 100 kHz with an amplitude of 0.01 V.

4.4 C-R-C load test

After the PCB was assembled, a test was done without electrodes to ascertain whether the system works in principle. To mimic perfectly polarizable electrodes, capacitors are used. The media fluid is modelled as a resistor. The component values where arbitrarily chosen at 10 µF for the capacitors and 100 Ω for the resistor. Then, the PCB was configured to output two 50 µs pulses with an amplitude of 50 mA and discharge in the negative phase with -75 mA DC. Repeating the sequence every 550 µs or at 1.8 kHz. The results of this test can be seen in Figure 15. On the left of the grid, the red line indicates the amplitude as a voltage measurement over the 100 Ω resistor. It shows that the output stage can produce the right amplitude and timing. However, the most obvious thing in these graphs is the mess

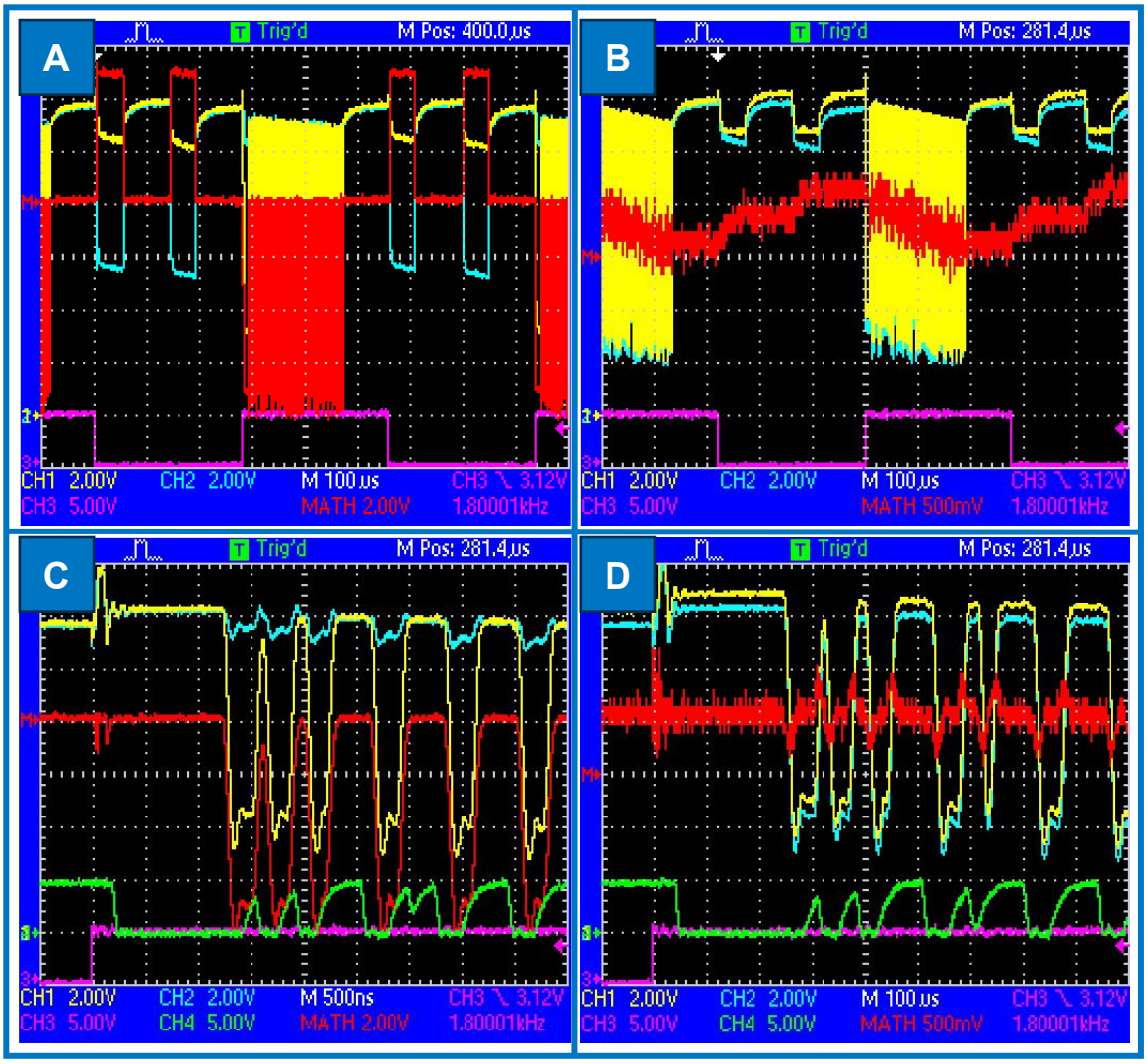

Figure 15: Scope test results from the C-R-C load test. A: The red line is the calculated voltage difference between the yellow and blue lines (top and bottom of 100 Ω resistor load). It is a measure of the current flowing through the load. B: The red line is the calculated voltage difference between the yellow and blue lines (top and bottom of the anodic work electrode). It is a measurement of the charge on the anodic capacitor. C: A zoomed in version of A where the output during the negative phase can be seen. D: A zoomed in version of B where the interference on the capacitor voltage can be seen during negative phase stimulation. The green lines in C and D indicate the output of the comparator measuring the "electrode" voltage. The purple line in all plots is the polarity control signal. The scope is triggered on this signal. A logic high (5 V) means negative stimulation and a logic low (0 V) means positive stimulation.

that is the negative phase. This should be a constant current until the charge on the electrode reaches zero where stimulation should stop. Instead, crossing into the negative part of stimulation, the polarity swaps and the blue and yellow lines (the top and bottom of the resistor in the left graphs) swap places. This swap, together with the relatively long wires produce some interference which in turn makes the charge measurement briefly zero as shown in Figure 15D (the red line). This causes the comparator to give the signal to stop stimulation, as can be seen by the green line. When the stimulation stops, the charge measurement returns to its true value, and the comparator stops giving the signal to stop stimulation. Which causes the change in common mode voltage on the H-bridge, which causes interference, and the loop continues. This oscillation is happening at a frequency that corresponds to the reaction time of the comparator and H-bridge switches and is undesirable. A solution to the problem would be to use some memory element like a flipflop to keep the stimulation turned off when the comparator detects the zero crossing until the next cycle begins. However, care must be taken to not allow too much interference as it could result in a lot of charge to be left on the electrode.
Another apparent problem is that the comparator has a small bias current. Which discharges the electrode it's measuring. This causes that electrode to be at zero charge slightly earlier than the other electrode allowing for a voltage to build up on that electrode. The small amount of voltage that remains after the stimulation cycle builds up on every cycle and over the course of a couple of seconds, the voltage on the unobserved electrode exceeds one volt.

4.5 Electric field testing in electrolyte

Due to time limitations, no specific channel shape was made to do this test. So, the two working electrodes were submerged in PBS together with the stainless-steel measurement electrode. However, due to the shape of the well, the charge measurement was drowned out by the voltage build up over the fluid due to stimulation so no conclusions could be made about the charge balancing circuit. While the timing of the pulses were equivalent to the C-R-C model, the amplitude was difficult to verify as it would require the knowledge of the equivalent resistance between the two working electrodes.

5 Discussion

This work presents the ability to create a circuit small enough to fit under the footprint of a 48-well plate which can stimulate all 48 wells with independent stimulation configurations. The configuration circuitry allows to configure the amplitude values for both negative and positive stimulation per row. While also providing a way to set any square wave timing sequence with variable on and off time for both sides of stimulation per column. As well as control over how often the waveform repeats before the polarity switches. This configuration can then be translated into the proper current controlled stimulation through an output stage small enough to fit under a single well of a 48-well plate while still leaving room to view the cells through a cutout slit in the PCB.

However, the charge balancing scheme does not work in its current form and should be reworked before this device can be used to stimulate cells. The measurement of the charge is very dependent on the channel shape; the comparator measuring one electrode causes charge to build up on the other electrode and the current state of the circuit allows for oscillation due to interference and noise.

Apart from the main problem that needs to be solved with this design, the charge balancing scheme, there are some other recommendations for future work. The user interface is currently a bundle of pin headers and jumpers that requires some math to be usable. Although a manual could be written, it would be more user friendly to change the pin header and jumpers for digital chips like multiplexers and shift registers. This would in all likelihood not increase the size or cost of the design but would allow the user to interface with the device through some microcontroller. This could either be done with a USB cable and a computer interface, or a screen and buttons on the device itself. In this case, the microcontroller or computer could make the necessary calculations to turn the desired configuration in the right instructions for the multiplexers and shift registers. Easing the burden on the user.

Additionally, the current amplitude scale could be improved upon by seeking a method that would match the desired exponential scale better than the current solution. A more complex circuit that uses a diode to get the exponential behaviour could possibly be conceived.

Lastly, the current design is quite compact in components on the output stage side. The components chosen in this work were chosen in such packages that soldering by hand was still an option. It would be possible to get many if not all components in smaller sizes and getting the PCB assembled by an external company or soldered using an oven. This would remove the ability to easily troubleshoot the design but could increase the number of channels available or increase the size of the see through slits.

Bibliography

[1] M. Rabbani, E. Rahman, M. B. Powner, and I. F. Triantis, 'Making Sense of Electrical Stimulation: A Meta-analysis for Wound Healing', *Ann. Biomed. Eng.*, vol. 52, no. 2, pp. 153–177, Feb. 2024, doi: 10.1007/s10439-023-03371-2.

[2] S. N. Iwasa *et al.*, 'Novel Electrode Designs for Neurostimulation in Regenerative Medicine: Activation of Stem Cells', *Bioelectricity*, vol. 2, no. 4, pp. 348–361, Dec. 2020, doi: 10.1089/bioe.2020.0034.

[3] S. Hasiba-Pappas *et al.*, 'Does Electrical Stimulation through Nerve Conduits Improve Peripheral Nerve Regeneration?—A Systematic Review', *J. Pers. Med.*, vol. 13, no. 3, Art. no. 3, Mar. 2023, doi: 10.3390/jpm13030414.

[4] P. J. Nicksic *et al.*, 'Electronic Bone Growth Stimulators for Augmentation of Osteogenesis in In Vitro and In Vivo Models: A Narrative Review of Electrical Stimulation Mechanisms and Device Specifications', *Front. Bioeng. Biotechnol.*, vol. 10, Feb. 2022, doi: 10.3389/fbioe.2022.793945.

[5] R. Das, S. Langou, T. T. Le, P. Prasad, F. Lin, and T. D. Nguyen, 'Electrical Stimulation for Immune Modulation in Cancer Treatments', *Front. Bioeng. Biotechnol.*, vol. 9, Jan. 2022, doi: 10.3389/fbioe.2021.795300.

[6] J. J. Vaca-González, J. M. Guevara, J. F. Vega, and D. A. Garzón-Alvarado, 'An In Vitro Chondrocyte Electrical Stimulation Framework: A Methodology to Calculate Electric Fields and Modulate Proliferation, Cell Death and Glycosaminoglycan Synthesis', *Cell. Mol. Bioeng.*, vol. 9, no. 1, pp. 116–126, Mar. 2016, doi: 10.1007/s12195-015-0419-2.

[7] G. Saulis, R. Rodaitė-Riševičienė, and R. Saulė, 'Cytotoxicity of a Cell Culture Medium Treated with a High-Voltage Pulse Using Stainless Steel Electrodes and the Role of Iron Ions', *Membranes*, vol. 12, no. 2, p. 184, Feb. 2022, doi: 10.3390/membranes12020184.

[8] J. Ehlich, Č. Vaščček, J. Dobeš, A. Ruggiero, M. Vejvodová, and E. D. Głowacki, 'Shattering the Water Window: Comprehensive Mapping of Faradaic Reactions on Bioelectronics Electrodes', *ACS Appl. Mater. Interfaces*, vol. 16, no. 40, pp. 53567–53576, Oct. 2024, doi: 10.1021/acsami.4c12268.

[9] D. C. Van Niekerk, 'Monitoring Tissue Function Dynamics in vitro with Bioelectronics: Towards Understanding Barrett's Oesophagus Pathogenesis', PhD Thesis, 2024. Accessed: Aug. 20, 2025. [Online]. Available: https://www.repository.cam.ac.uk/items/32d7f9f2-9f14-447e-bb9d-7b5b717b2c0a

[10] E. P. W. Jenkins, S. T. Keene, I. B. Dimov, P. Oldroyd, and G. G. Malliaras, 'High capacitance freestanding PEDOT:PSS electrodes for low-frequency electric field delivery', *AIP Adv.*, vol. 14, no. 3, p. 035006, Mar. 2024, doi: 10.1063/5.0180487.

[11] G. Dijk, H. J. Ruigrok, and R. P. O'Connor, 'Influence of PEDOT:PSS Coating Thickness on the Performance of Stimulation Electrodes', *Adv. Mater. Interfaces*, vol. 7, no. 16, p. 2000675, 2020, doi: 10.1002/admi.202000675.

[12] X. S. Zheng, C. Tan, E. Castagnola, and X. T. Cui, 'Electrode Materials for Chronic Electrical Microstimulation', *Adv. Healthc. Mater.*, vol. 10, no. 12, p. e2100119, Jun. 2021, doi: 10.1002/adhm.202100119.

[13] M. Verdes, K. Mace, L. Margetts, and S. Cartmell, 'Status and challenges of electrical stimulation use in chronic wound healing', *Curr. Opin. Biotechnol.*, vol. 75, p. 102710, Jun. 2022, doi: 10.1016/j.copbio.2022.102710.

[14] Y. J. Cheah, M. R. Buyong, and M. H. Mohd Yunus, 'Wound Healing with Electrical Stimulation Technologies: A Review', *Polymers*, vol. 13, no. 21, Art. no. 21, Jan. 2021, doi: 10.3390/polym13213790.

[15] R. Luo, J. Dai, J. Zhang, and Z. Li, 'Accelerated Skin Wound Healing by Electrical Stimulation', *Adv. Healthc. Mater.*, vol. 10, no. 16, p. 2100557, 2021, doi: 10.1002/adhm.202100557.

[16] Y. Zhang, S. Huang, Y. Cao, L. Li, J. Yang, and M. Zhao, 'New Opportunities for Electric Fields in Promoting Wound Healing: Collective Electrotaxis', *Adv. Wound Care*, May 2024, doi: 10.1089/wound.2024.0003.

[17] C. Chen, X. Bai, Y. Ding, and I.-S. Lee, ‘Electrical stimulation as a novel tool for regulating cell behavior in tissue engineering’, *Biomater. Res.*, vol. 23, no. 1, p. 25, Dec. 2019, doi: 10.1186/s40824-019-0176-8.
[18] S. Xie, J. Huang, A. T. Pereira, L. Xu, D. Luo, and Z. Li, ‘Emerging trends in materials and devices-based electric stimulation therapy for tumors’, *BMEMat*, vol. 1, no. 3, p. e12038, 2023, doi: 10.1002/bmm2.12038.
[19] S. Shaner *et al.*, ‘Bioelectronic microfluidic wound healing: a platform for investigating direct current stimulation of injured cell collectives’, *Lab. Chip*, vol. 23, no. 6, pp. 1531–1546, Mar. 2023, doi: 10.1039/D2LC01045C.
[20] K. Srirussamee, R. Xue, S. Mobini, N. J. Cassidy, and S. H. Cartmell, ‘Changes in the extracellular microenvironment and osteogenic responses of mesenchymal stem/stromal cells induced by in vitro direct electrical stimulation’, *J. Tissue Eng.*, vol. 12, p. 2041731420974147, Jan. 2021, doi: 10.1177/2041731420974147.
[21] J. Du *et al.*, ‘Optimal electrical stimulation boosts stem cell therapy in nerve regeneration’, *Biomaterials*, vol. 181, pp. 347–359, Oct. 2018, doi: 10.1016/j.biomaterials.2018.07.015.
[22] J. Leal, S. Shaner, N. Jedrusik, A. Savelyeva, and M. Asplund, ‘Electrotaxis evokes directional separation of co-cultured keratinocytes and fibroblasts’, *Sci. Rep.*, vol. 13, no. 1, Art. no. 1, Jul. 2023, doi: 10.1038/s41598-023-38664-y.
[23] K. Zhu, N. R. Hum, B. Reid, Q. Sun, G. G. Loots, and M. Zhao, ‘Electric Fields at Breast Cancer and Cancer Cell Collective Galvanotaxis’, *Sci. Rep.*, vol. 10, no. 1, p. 8712, May 2020, doi: 10.1038/s41598-020-65566-0.
[24] X. Ren *et al.*, ‘Keratinocyte electrotaxis induced by physiological pulsed direct current electric fields’, *Bioelectrochemistry*, vol. 127, pp. 113–124, Jun. 2019, doi: 10.1016/j.bioelechem.2019.02.001.
[25] Y.-J. Huang *et al.*, ‘Electrophoresis of cell membrane heparan sulfate regulates galvanotaxis in glial cells’, *J. Cell Sci.*, vol. 130, no. 15, pp. 2459–2467, Aug. 2017, doi: 10.1242/jcs.203752.
[26] Y.-J. Huang, G. Hoffmann, B. Wheeler, P. Schiapparelli, A. Quinones-Hinojosa, and P. Searson, ‘Cellular microenvironment modulates the galvanotaxis of brain tumor initiating cells’, *Sci. Rep.*, vol. 6, no. 1, p. 21583, Feb. 2016, doi: 10.1038/srep21583.
[27] D. J. Cohen, W. James Nelson, and M. M. Maharbiz, ‘Galvanotactic control of collective cell migration in epithelial monolayers’, *Nat. Mater.*, vol. 13, no. 4, pp. 409–417, Apr. 2014, doi: 10.1038/nmat3891.
[28] A. P. Mazzoleni, B. F. Sisken, and R. L. Kahler, ‘Conductivity values of tissue culture medium from 20°C to 40°C’, *Bioelectromagnetics*, vol. 7, no. 1, pp. 95–99, 1986, doi: 10.1002/bem.2250070111.
[29] A. Savva, S. Wustoni, and S. Inal, ‘Ionic-to-electronic coupling efficiency in PEDOT:PSS films operated in aqueous electrolytes’, *J. Mater. Chem. C*, vol. 6, no. 44, pp. 12023–12030, Nov. 2018, doi: 10.1039/C8TC02195C.